Spacecraft trajectories to the L point of the Sun–Earth three-body problem

Marco Tantardini, Elena Fantino, Yuan Ren, Pierpaolo Pergola, Gerard Gómez, Josep J. Masdemont

Celestial Mechanics and Dynamical Astronomy manuscript No.
(will be inserted by the editor)

Spacecraft trajectories to the L_3 point of the Sun-Earth three-body problem

Marco Tantardini · Elena Fantino · Yuan Ren · Pierpaolo Pergola · Gerard Gómez · Josep J. Masdemont

Received: date / Accepted: date

Abstract Of the three collinear libration points of the Sun-Earth Circular Restricted Three-Body Problem (CR3BP), L_3 is that located opposite to the Earth with respect to the Sun and approximately at the same heliocentric distance. Whereas several space missions have been launched to the other two collinear equilibrium points, i.e. L_1 and L_2, taking advantage of their dynamical and geometrical characteristics, the region around L_3 is so far unexploited. This is essentially due to the severe communication limitations caused by the distant and permanent opposition to the Earth, and by the gravitational perturbations mainly induced by Jupiter and the close passages of Venus, whose effects are more important than those due to the Earth. However, the adoption of a suitable periodic orbit around L_3 to ensure the necessary communication links with the Earth, or the connection with one or more relay satellites located at L_4 or L_5, and the simultaneous design of an appropriate station keeping-strategy, would make it possible to perform valuable fundamental physics and astrophysics investigations from this location. Such an opportunity leads to the need of studying the ways to transfer a spacecraft (s/c) from the Earth's vicinity to L_3. In this contribution, we investigate several trajectory design methods to accomplish such a transfer, i.e., various types of two-burn impulsive trajectories in a Sun-s/c two-body model, a patched conics strategy exploiting the gravity assist of the nearby planets, an approach based on traveling on invariant manifolds of periodic orbits in the Sun-Earth CR3BP, and finally a low-thrust transfer. We examine advantages and drawbacks, and we estimate the propellant budget and time of flight (TOF) requirements of each.

Keywords Two-Body Problem · Patched Conics · Gravity Assist · Circular Restricted Three-Body Problem · Libration Points · Periodic Orbits · Invariant Manifolds · Low-Thrust

1 Introduction

A space observatory placed at or around L_3 could provide insight into local astrophysical phenomena such as the solar wind and the properties of the Sun's magnetosphere; it could monitor the evolution of the sunspots, perform solar storm forecast and observe the space environment from a new perspective, hidden to the Earth, and in this way supplement and complete the information obtainable, e.g., from L_1 or from Earth based observatories. A satellite at L_3 could be even thought of as part of a circular or spherical constellation of s/c monitoring the Sun's activity and the space environment at many different angles. Moreover, L_3 may constitute a privileged site to perform relativity experiments, such as measuring the gravitational bending of light on behalf of the Sun, as a follow-up of the Cassini-Huygens radio science observations. Finally, some minor bodies such as NEOs and comets, hidden by the Sun as viewed from Earth, could be observed and even tracked from this more favorable location.

Marco Tantardini
Departament de Matemàtica Aplicada I, ETSEIB, Universitat Politècnica de Catalunya, Diagonal 647, 08028 Barcelona, Spain. On leave from the Faculty of Aerospace Engineering, Delft University of Technology, Delft, The Netherlands
E-mail: marco.tantardini@gmail.com

Elena Fantino · Yuan Ren · Josep J. Masdemont
IEEC & Departament de Matemàtica Aplicada I, ETSEIB, Universitat Politècnica de Catalunya, Diagonal 647, 08028 Barcelona, Spain
E-mail: elena.fantino@upc.edu, yuan.ren@upc.edu, josep@barquins.upc.edu

Pierpaolo Pergola
Faculty of Computer Science, Electrical Engineering and Mathematics, University of Paderborn, Warburger Str. 100, D-33095, Paderborn, Germany
E-mail: pergola@math.uni-paderborn.de

Gerard Gómez
IEEC & Departament de Matemàtica Aplicada i Anàlisi, Universitat de Barcelona, Gran Via 585, 08007 Barcelona, Spain
E-mail: gerard@maia.ub.es

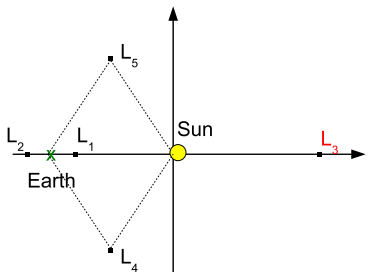

Fig. 1 The synodical barycentric reference frame of the Sun-Earth CR3BP showing the location of the two primaries and the five libration points.

The framework in which the L_3 point is defined is the CR3BP, which describes the motion of a massless particle in the gravitational force field created by two main bodies, the primaries, in Keplerian circular motion around their centre of mass. In the so-called synodical barycentric reference frame, the two primaries occupy fixed positions on the x-axis and there exist five equilibrium points for the third body to stay at rest (Fig. 1): in particular, the position of the three collinear points on the x-axis of the system are found by solving the Lagrange quintic equation ([11], pp. 134-138), which for L_3 provides the approximation 1.0000013 AU for the x coordinate of Fig. 1 when the mass ratio μ of the Sun-Earth CR3BP is given a value of $3.0404234 \cdot 10^{-6}$. L_3 orbits the Sun at a distance of 0.9999982 AU, hence on a slightly inner orbit with respect to that of the Earth.

Thinking of a space mission to L_3, necessarily introduces the issue of designing the transfer trajectory from the Earth to this new destination. This problem is here investigated by considering several dynamical models and design methods and discussing preliminary solutions thus obtained. Note that if one neglects the small difference in the orbital radii between the Earth and L_3 in heliocentric inertial space, this transfer is essentially a 180° re-phasing problem, i.e., providing the s/c orbit with a true anomaly difference of 180° with respect to the Earth.

Section 2 presents three design strategies based on the use of impulsive maneuvers in the Sun-s/c two-body problem. This is followed (Sect. 3) by a survey of optimized planetary gravity assisted solutions based on the patched conics method. In Sect. 4 the invariant manifolds of planar Lyapunov orbits around the three collinear libration points are used to reach the vicinity of L_3. Sect. 5 investigates two low-thrust strategies, based on optimizing the transfer time with a continuously operating thrust and the fuel consumption in a thrust-coast-thrust operation scheme, respectively. Finally, Sects. 6 and 7 summarize and compare our findings. For a comprehensive description of the present investigation the reader is referred to [12].

2 Two-body impulsive maneuvers

The model is the planar Sun-s/c two-body problem, with the s/c departing from the Earth's heliocentric orbit and reaching L_3 with zero relative speed. Four solution types, made of Keplerian elliptical arcs and impulsive maneuvers, are here presented.

2.1 Bi-elliptic transfer

A bi-elliptic transfer (Fig. 2a) is a classical three-burns maneuver consisting of two half elliptical orbits: from the initial orbit of radius r_a, a ΔV_a is applied boosting the s/c into the first transfer orbit with an (arbitrary) apoapsis at some point r_b away from the central body. At this point, a second burn, of size ΔV_b, is applied sending the s/c into the second elliptical orbit with periapsis at the radius r_c of the final desired orbit where a third ΔV_c is performed for injection (see, e.g., [13], pp. 324-332).

The requirement that the arrival point on the target orbit be in opposition to the Earth can be expressed as a relation between the sum of the transfer times on the two elliptical orbits and the orbital period $T_\oplus$ of the Earth:

$$\pi\sqrt{\frac{(r_a+r_b)^3}{8GM_\odot}}+\pi\sqrt{\frac{(r_b+r_c)^3}{8GM_\odot}}=\frac{n}{2}T_\oplus, \quad n=1,3,5,... \tag{1}$$

thus providing the distance r_b. In Eq. 1, $GM_\odot$ is the gravitational parameter of the Sun. By varying the odd integer n, r_b and the corresponding ΔV budget and transfer time are obtained (Fig. 3a): the cheapest solution (with a ΔV of 6.7 km s^{-1}) is obtained for $n = 3$ which corresponds to a reasonably short transfer time (1.5 years). Note that, when the transfer occurs between two circular orbits which are very close to each other, like in this case, the size of the apoapsis maneuver is very small. At the limit in which the departure and target orbits are identical, the apoapsis maneuver disappears and the resulting transfer implies two tangential burns, shown in Fig. 2b.

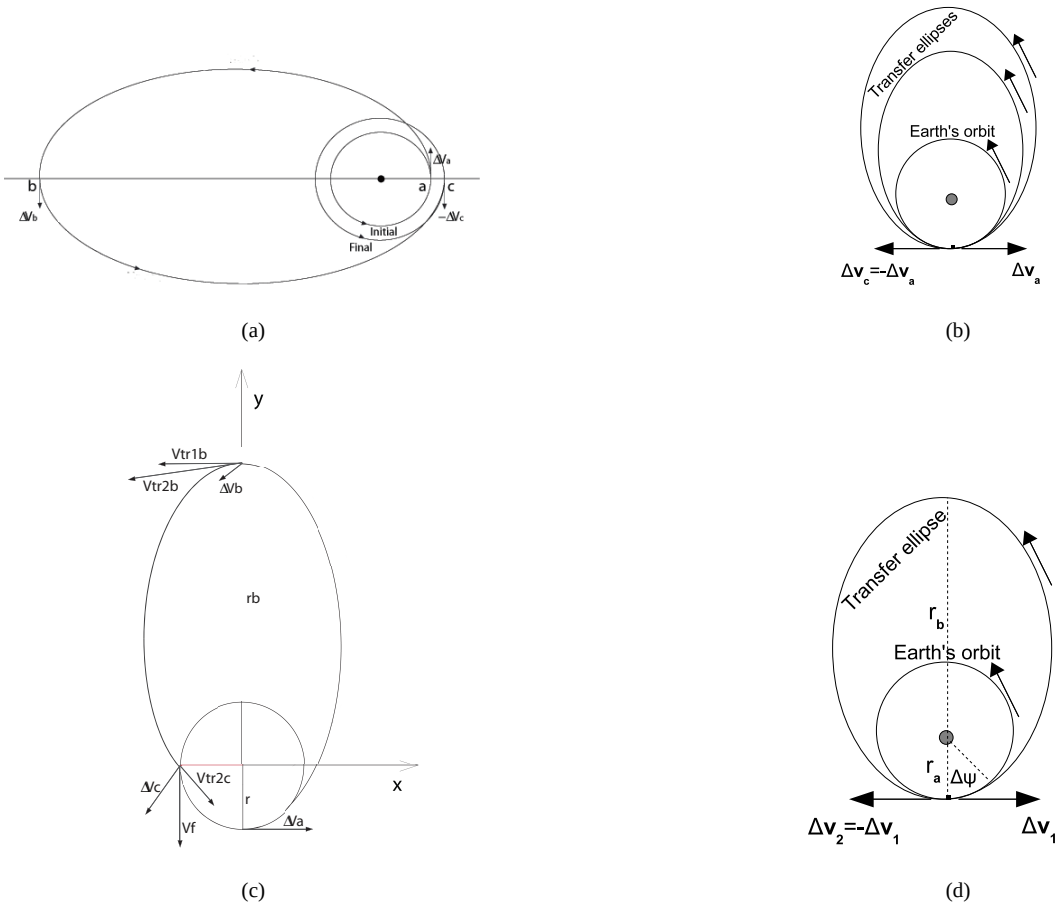

Fig. 2 Types of two-body impulsive maneuvers trajectories from the Earth's orbit to L_3: a classical bi-elliptic (a), its limiting case, called two-tangent burn maneuver, for equal departure and arrival orbits (b), a bi-elliptic one-tangent burn (c), a multi-revolution orbit (d).

2.2 Bi-elliptic one-tangent burn transfer

A generalization of the previous case is obtained by imposing that the total transfer angle $\Delta\phi$ is in the interval $]\pi,2\pi]$ (see also [13], pp. 333-338 for a similar maneuver). The trajectory is a sequence of two elliptical arcs: the first is half of an ellipse, thus involving a π radians transfer angle, whereas the second subtends an angle of $\Delta\phi - \pi$. The total transfer requires three impulses, but, whereas the first, ΔV_a, is applied tangentially, the remaining two, ΔV_b and ΔV_c, are in the direction required to perform the insertion onto the second elliptical arc and the target orbit, respectively (see Fig. 2c). The apoapsis distance r_b and the transfer angle $\Delta\phi$ must be *a priori* set. Then, the timing requirement between the position of the Earth on its orbit and that of L_3 on arrival leads to a relation between the sum of the times T_{e1} and T_{e2} spent on the two elliptical arcs and the period $T_\oplus$ of the Earth:

$$T_{e1} + T_{e2} = \left(\frac{\Delta\phi - \pi}{2\pi}\right) T_\oplus + nT_\oplus, \quad n = 0, 1, 2, 3, ... \tag{2}$$

with

$$T_{e1} = \pi\sqrt{\frac{(r_a + r_b)^3}{8GM_\odot}}. \tag{3}$$

For a given n, Eq. 2 provides the value of T_{e2} which is then used to solve the Lambert problem on the second arc, thus allowing to compute ΔV_b and ΔV_c as the difference of the velocities at the start and end points of such arc with the velocity at apoapsis of the first ellipse and the velocity of the target circular orbit, respectively.

The case here considered corresponds to a total transfer angle $\Delta\phi$ of 270°. Several values for the apoapsis radius r_b between 0.7 and 1.7 AU have been adopted leading to very expensive ($\gg$ 10 km s^{-1}) and therefore unfeasible solutions. The cheapest corresponds to an apoapsis radius r_b of 1.7 AU and requires a total ΔV of 16.9 km s^{-1} and a TOF of 1 year and 3 months.

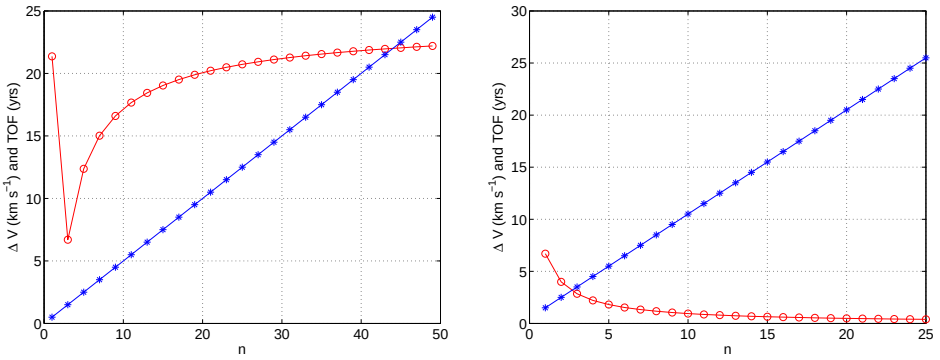

Fig. 3 ΔV budget (open circles) and TOF (stars) for the bi-elliptic (a) and multi-revolution (b) strategies as a function of the odd integer n on which the timing problem is designed.

2.3 Multi-revolution transfer

Finally, one can think of a multi-orbit transfer, which consists in following one and the same transfer ellipse many times in such a way that every revolution dephases the s/c of a given (small) angle $\Delta\psi$ with respect to the Earth. This option requires two tangential burns of equal size, the first one to insert into the multi-revolution ellipse and the second one to leave it and place the s/c on the target orbit. $\Delta\psi$ determines the integer number n (n = 1,2,3,...) of revolutions to be performed in order to acquire the desired π displacement with respect to the Earth (here L_3 and the Earth are assumed to be on the same heliocentric orbit), and the total transfer time T_m:

$$n = \frac{\pi}{\Delta\psi}, \tag{4}$$

$$T_m = \frac{2n+1}{2} T_{\oplus}. \tag{5}$$

Therefore, the displacement $\Delta\psi$ determines the apoapsis distance r_b of the transfer ellipse through its period T_e:

$$T_e = \frac{T_m}{n}, \tag{6}$$

$$r_b = 2a - r_a, \tag{7}$$

in which a is the semi-major axis of the transfer ellipse. Finally, the ΔV budget is twice the magnitude of the impulse given to insert into the transfer ellipse and can be represented as a function of n as shown in Fig. 3b where also the TOF is given: the smaller the angle $\Delta\psi$, the lower the total cost and the longer the transfer.

3 Gravity assisted trajectories

An optimized three-dimensional (3D) patched conics strategy exploiting the gravity assist of the nearby planets is here investigated as the natural evolution of the impulsive maneuver solution of the preceding section. L_3 is geometrically defined as an anti-Earth, i.e., it has the same ephemerides as the Earth, except for a true anomaly difference of 180°.

According to the patched conics method, a trajectory to reach L_3 is divided into segments, the end points of which are planetary swingbys or departure and arrival events. Each trajectory segment is modeled as a Sun-s/c two-body problem, whereas at the swingby events (assumed to be instantaneous) the encounter with the planet inside the planet's sphere of influence is modeled as a planet-s/c two-body problem. Note that L_3 is treated by the algorithm as an arrival planet of zero mass (i.e., no swingby occurs) and therefore the arrival maneuver simply circularizes the orbit. Impulsive maneuvers are allowed at departure (ΔV_d), arrival (ΔV_a) and at the swingbys: one impulse at periapsis of size ΔV_{GA} is allowed in order to fill the difference between the periapsis velocities of the incoming and the outgoing hyperbolic paths, determined by the arrival and departure heliocentric velocities at the surface of the sphere of influence and by the constraint of connecting in position space at a common pericenter. No deep space maneuvers are allowed. On each interplanetary segment the trajectory is determined by solving a 3D Lambert problem between two dates and two heliocentric position vectors.

The trajectory solution is an optimization problem in which the planetary encounters and their ordering are given *a priori*. The departure date, the arrival date (and hence the corresponding position vectors, as determined by the planetary ephemerides based on polynomials in terms of the classical orbital elements, see [13], pp. 297-300 and 995-999) and the dates of the planetary

swingbys are varied in order to minimize an objective function C defined as the sum of the magnitudes of the maneuvers, with the inclusion of a penalty function:

$$C = \Delta V_d + \Delta V_a + \sum_{i=0}^{n} \left[\Delta V_{GAi} + W_i \cdot \frac{(R_{Pi} + h_{min\ i} - r_{\pi i})^2}{R_{Pi}^2} \right]. \tag{8}$$

Here n is the number of swingbys and ΔV_{GAi} is the magnitude (equal to zero for unpowered swingbys) of the periapsis maneuver at the i^{th} encounter. An additional cost, i.e., the penalty function, appears in Eq. 8 through the second term in the sum and is represented as a nonlinear expression involving the radius R_{Pi} of the encountered planet, the minimum swingby altitude $h_{min\ i}$ and the actual value of the periapsis distance $r_{\pi i}$ computed by the swingby solver. W_i is a weight and increases from preliminary search (~ 10) to local optimizations (~ 100) to guarantee the feasibility of the final solutions. It is worth noting that this penalty function is zero whenever the minimum altitude constraint is satisfied by the current solution, i.e., $r_{\pi i} > R_{Pi} + h_{min\ i}$.

This local optimization problem is solved through a sequential quadratic programming algorithm fed with initial guesses for the optimization variables, obtained by a global optimization method: a genetic algorithm or a discrete search grid on a range of dates. Typically, the former global method is adopted when the trajectory involves many ($n \geq 3$) swingbys, the latter being preferred for problems of small size ($n = 1$ or $n = 2$).

Several solutions have been explored by varying the number and ordering of the planetary swingbys, with the encountered bodies chosen among the nearest planets, i.e., Mercury, Venus, Earth and Mars. Table 1 summarizes the results with an acceptable cost, i.e. less than 15 km s^{-1}, and for each planetary sequence it gives the minimum ΔV budget found (given as the sum of the individual impulses), an estimate of the gravity assist ΔV_B provided by the planets (expressed as the sum of the individual contributions) and the corresponding TOF (sum of the times spent on each segment). Solutions involving swingbys at Mercury or more than two intermediate encounters have been tested, but the resulting trajectories are very expensive and, therefore, do not appear in this list.

The optimized solution of the type Earth-Earth-L_3 (EEL_3) is the cheapest (3.80 km s^{-1}) of all. With a transfer time of 1.5 years from the Earth's gravity assist to arrival at L_3, it is geometrically identical to the two-tangent burn maneuver with $n = 3$, the reduction in cost being ensured by the Earth's gravity assist which provides a natural ΔV_B of 2.8 km s^{-1}. However, this solution is characterized by very low (< 0.5 km s^{-1}) incoming and outgoing relative velocities at the surface of the Earth's sphere of influence, which cause the swingby to be too slow to be considered instantaneous, contrary to what the model requires. This could make this solution unrealistic (or at least requiring verification in an n-body model) unless appropriately modified, for example, by introducing deep space maneuvers.

From this preliminary analysis, the best solution appears to be that involving one swingby at the Earth, because sending the s/c to an inner or an outer planet for subsequent re-direction to a heliocentric distance of 1 AU, implies a higher cost. Alternatively, and aiming at encountering the Earth at the same departure location but avoiding heliocentric orbits with large semi-major axis (which are expensive to reach and leave), we have investigated what we called the Earth resonant swingby. This option introduces additional, multiple revolutions on two intermediate (i.e., between departure and Earth's swingby, and between Earth's swingby and arrival, respectively) elliptical orbits with semi-major axis determined by the the chosen resonance and close to that of the Earth's orbit. The numbers n_1 and n_2 of revolutions on the two elliptical, resonant orbits are integer and are chosen by means of a grid search. An important characteristic of this type of solutions is that the s/c encounters the Earth in a swingby with adequate dynamical parameters and reaches L_3 with a small insertion maneuver[1]. Of course, the price is a much extended TOF with respect to the standard solution. Two examples of this type are labelled in Table 1 by $En_1r_1En_2r_2L_3$, and are illustrated in Fig. 4a (where $n_1 = 4$ and $n_2 = 2$) and 4b (in which $n_1 = 2$ and $n_2 = 2$).

A direct Earth-L_3 transfer again geometrically coincides with the two-tangent burn solution with $n = 3$. Finally, illustration of the best solutions obtained for the sequences Earth-Mars-L_3 (EML_3) and Earth-Venus-Venus-Earth-L_3 ($EVVEL_3$) are given in Fig. 5a and 5b, respectively.

4 Invariant manifold transfers

The dynamics of the stable and unstable invariant manifold tubes associated to the L_1 and L_2 periodic orbits in the CR3BP has been successfully applied to the design of s/c transfers (e.g., the Genesis [8] or the Herschel/Planck missions [6]). This suggests that perhaps also the dynamics of the invariant manifolds of periodic orbits around L_3 in the Sun-Earth CR3BP may be exploited for designing a low-cost transfer from the Earth to this new destination. In this work, a family of 74 planar Lyapunov periodic orbits around L_3 is considered as target of the transfer: the x amplitude of the orbits ranges from 10^{-4} to 10^{-1} AU, which corresponds to y amplitudes of up to 0.25 AU, thus including a considerable number of orbits large enough (i.e., > 0.1

[1] It is worth noting that these trajectories are, in first approximation, independent from the departure date: a change in the launch date results only in a rotation of the solution because of the resonances and the L_3 location.

Table 1 Optimized gravity assisted solutions: for each given planetary sequence we report the minimum ΔV budget found (given as the sum of the individual impulses), the gravity assist ΔV_B provided by the bodies (expressed as the sum of the individual contributions) and the corresponding TOF (sum of the times spent on each segment). The meaning of the symbols used to name the planetary sequences is the following: E = Earth, V = Venus, M = Mars.

Pl. seq.	$\Delta V = \Delta V_d + \sum_{i=1}^{n} \Delta V_i + \Delta V_a$ (km s^{-1})	$\Delta V_B = \sum_{i=1}^{n} \Delta V_{Bi}$ (km s^{-1})	$TOF = \sum_{i=1}^{n} (TOF)_i + (TOF)_a$ (days)
EEL_3	3.80 = 0 + 0.51 + 3.29	2.80	586 = 39 + 547
$E4r_1E2r_2L_3$	4.72 = 2.49 + 0.08 + 2.15	4.13	2674 = 1460 + 1214
$E2r_1E2r_2L_3$	4.95 = 2.60 + 0.08 + 2.27	4.31	2321 = 1440 + 881
EL_3	6.57	–	548
EML_3	6.26 = 3.22 + 0 + 3.04	0.01	560 = 341 + 219
$EVVEL_3$	6.94 = 3.00 + 0.07 + 0.02 + 0.12 + 3.73	18.57 = 6.25 + 6.34 + 5.98	1248 = 172 + 449 + 115 + 512
$EVEML_3$	7.89 = 3.37 + 0 + 0 + 0 + 4.52	10.77 = 4.70 + 3.40 + 2.67	1080 = 135 + 266 + 333 + 346
EVL_3	16.03 = 3.15 + 0.45 + 12.43	7.66	586 = 106 + 480
$EMEL_3$	9.85 = 5.15 + 0 + 0.86 + 3.84	2.40 = 0.02 + 2.38	1236 = 114 + 611 + 511
$EMVL_3$	11.65 = 4.95 + 1.09 + 2.11 + 3.50	8.18 = 3.76 + 4.42	757 = 163 + 416 + 178
$EVEL_3$	11.80 = 7.91 + 0 + 0.11 + 3.78	13.01 = 6.87 + 6.14	859 = 250 + 95 + 514
$EVML_3$	12.82 = 3.88 + 0 + 2.53 + 6.41	9.27 = 7.16 + 2.11	737 = 123 + 345 + 269
$EVVL_3$	14.40 = 10.79 + 0 + 0.59 + 3.02	10.22 = 4.14 + 6.08	964 = 386 + 433 + 145

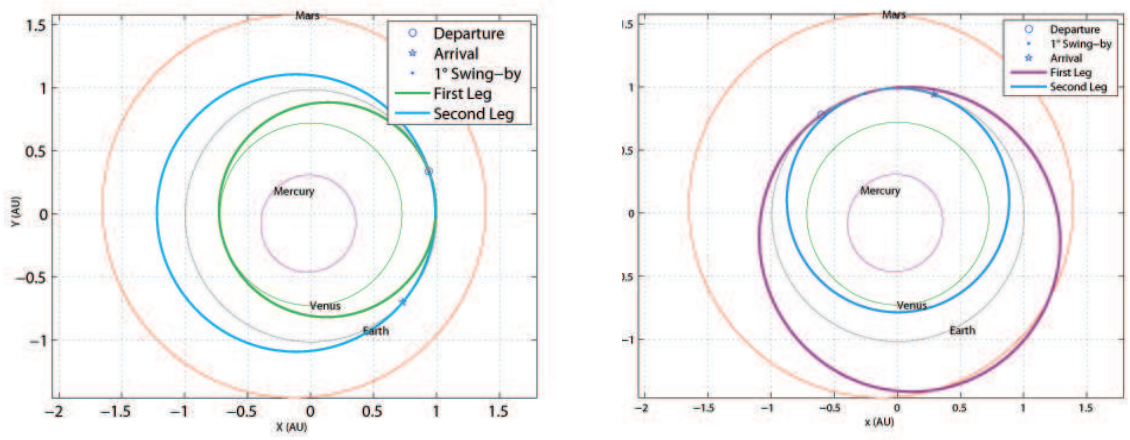

(a) (b)

Fig. 4 Two types of $En_1r_1En_2r_2L_3$ solutions: an $E4r_1E2r_2L_3$ (a), and an $E2r_1E2r_2L_3$ (b).

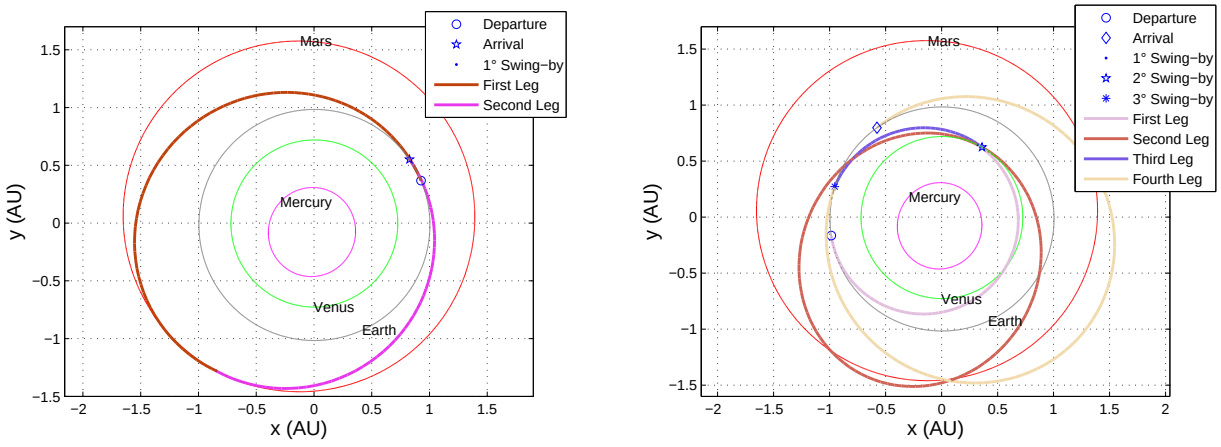

(a) (b)

Fig. 5 Optimized trajectories of the type EML_3 (a) and $EVVEL_3$ (b).

AU in y) to ensure visibility from the Earth. From the largest to the smallest orbit, the Jacobi constant[2] spans the range from 2.985554 to 3.000006. The adoption of Halo orbits as alternative destinations might benefit from the three-dimensionality of these objects. However, the study of the transfer strategy by means of invariant manifolds, the cost and TOF budgets would not differ significantly from the planar case. The adoption of planar orbits therefore ensures sufficient generality while simplifying the problem by neglecting the third dimension.

The mass ratio μ of the Sun-Earth CR3BP falls into the range of values for which the stable and unstable invariant manifolds of the Lyapunov orbits around L_3 are known to perform so-called horseshoe motion ([1,3]), flowing above and below the x-axis of the system towards the Earth (but never reaching it) and then bouncing back to the progenitor orbit (Fig. 6). Unfortunately, the transfer times to the closest approach with the Earth (between 0.2 and 0.4 AU over the family) are so large that these trajectories must be necessarily discarded for s/c applications: depending on the size of the Lyapunov orbit in the given family, these times range from 700 to 800 years.

A much more realistic alternative is obtained by following the approach devised by [7] which consists in considering the orbits belonging to the unstable manifolds of Lyapunov orbits around either L_1 or L_2 in the Sun-Earth system: Fig. 7a shows that at typical energy levels for which the Earth's lobe determined by the zero velocity curves opens on both sides, the unstable manifolds of planar Lyapunov orbits around L_1 after traveling through the Hill's sphere containing the Sun, cross the x-axis close to L_3, whereas the unstable manifolds of planar Lyapunov orbits around L_2 approach L_3 from outer space. Both types flow close to the forbidden region and bounce several times off the zero-velocity curve that confines it (Fig. 7). On approaching L_3, the orbits of these manifolds pass through the area where also the Lyapunov orbits of the L_3 family exist (Fig. 8). The existence of such overlap, in configuration space, can be exploited to design a transfer to L_3 through either L_1 or L_2: the s/c could perform a multi-objective mission by first visiting L_1 or L_2 and then, following a trajectory belonging to one of the associated unstable invariant manifolds, reach the region around L_3 and finally be inserted into a Lyapunov orbit of the target family (see also [9,5]). The whole invariant manifold flight would take between 5 and 12 years. The final insertion, in general, requires an impulsive maneuver which, by the way, corresponds to unclosing the forbidden region around L_3 and raising the energy of the approaching trajectory to match that of the selected target Lyapunov orbit. The orbit insertion maneuver is designed to occur at the intersection of the incoming trajectory with the x-axis. We report here the results for one solution of the type L_1-L_3 and one solution of the type L_2-L_3. In both cases, the departure Lyapunov orbit has x-amplitude of approximately 0.006 AU and y-amplitude of about 0.016 AU and is sampled with 200 points. The Jacobi constant values on the departure orbits are of 3.000690 and 3.000687, respectively. The local approximation of the unstable manifold associated to each orbit is obtained by application of a small perturbation in the direction of the unstable eigenvector and is then globalized by numerical integration during the time required to cut the selected Poincaré section at $y = 0$. There, the x interval of overlap between the manifold trajectories and the L_3 Lyapunov family is determined and at each incoming manifold trajectory one Lyapunov orbit is associated, that endowed with the nearest x coordinate at $y = 0$. Note that in general the same Lyapunov orbit can be associated to more manifold trajectories, with different inclinations with respect to the x-axis. The velocity correction ΔV to be applied for orbit insertion is given by

$$\Delta V = \sqrt{\dot{x}_M^2 + (\dot{y}_{L_3} - \dot{y}_M)^2}, \tag{9}$$

where $\dot{x}_M$ and $\dot{y}_M$ are the x and y components of the arrival velocity on the manifold trajectory and $\dot{y}_{L_3}$ is the only non-zero component of the velocity on the Lyapunov orbit at $y = 0$ due to the geometrical symmetry of such orbits with respect to the x-axis. The ΔV required for orbit insertion as a function of the x coordinate on the incoming manifold is illustrated in Fig. 9a and 9b, respectively for the L_1-L_3 and L_2-L_3 solutions. These plots provide estimates of the minimum and maximum size of the insertion maneuver from a given invariant manifold into the target L_3 family when the insertion point is at $y = 0$. The magnitude ranges found are almost identical (from 0.5 to 1.6 km s^{-1}) for the two cases considered, i.e., L_1-L_3 and L_2-L_3, with the latter extending a little bit more than the former. Note that with a ΔV of approximately 3 km s^{-1}, the s/c can be inserted into the stable manifold of a Lyapunov orbit around either L_1 or L_2 from a geostationary transfer orbit (GTO). As far as the transfer times are concerned, the GTO to L_1 or L_2 part of the trajectory can be covered in three months, whereas the manifold part of the transfer takes from 5.5 to 10.5 years for the L_1-L_3 solution (Fig. 10a) and from 6 to 11 years for the L_2-L_3 option (Fig. 10b).

5 Low-thrust trajectories

As an alternative to the design methods involving impulsive maneuvers, one can think of flying a s/c to L_3 with an electrical low-thrust engine. In our investigations the dynamical model adopted is the planar Sun-s/c two-body problem in which the equations of motion are:

$$\ddot{x} = -\frac{GM_\odot}{r^3}x + \frac{T}{m}\alpha_x, \tag{10}$$

[2] The definition adopted for the Jacobi constant is $J = x^2 + y^2 - 2\mu/r_1 + 2(\mu-1)/r_2 - \mu(\mu-1) - \dot{x}^2 - \dot{y}^2$, with μ the mass ratio of the system, x, y, $\dot{x}$ and $\dot{y}$ the synodical barycentric components of position and velocity of the third body, and r_1 and r_2 its distances from the first and second primary, respectively.

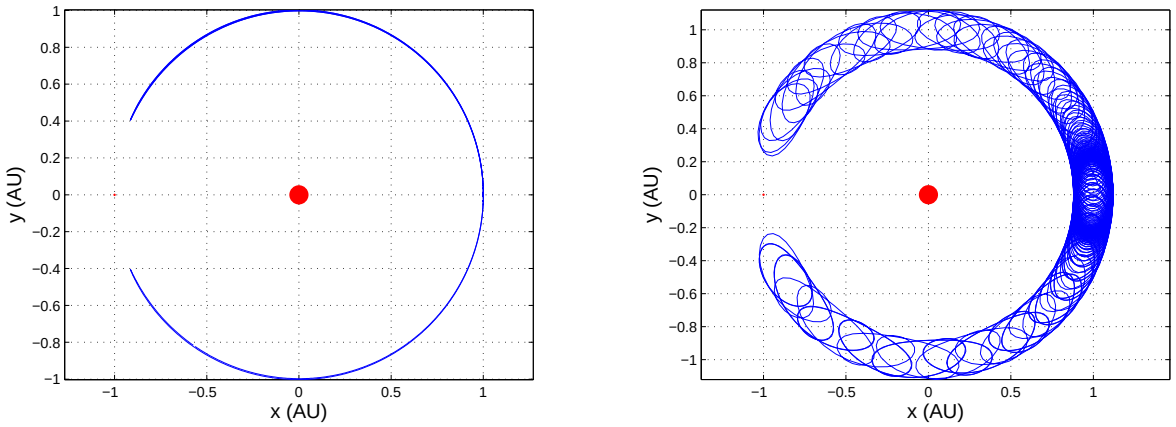

Fig. 6 The stable invariant manifolds of the smallest (a) and largest (b) Lyapunov orbits of the family.

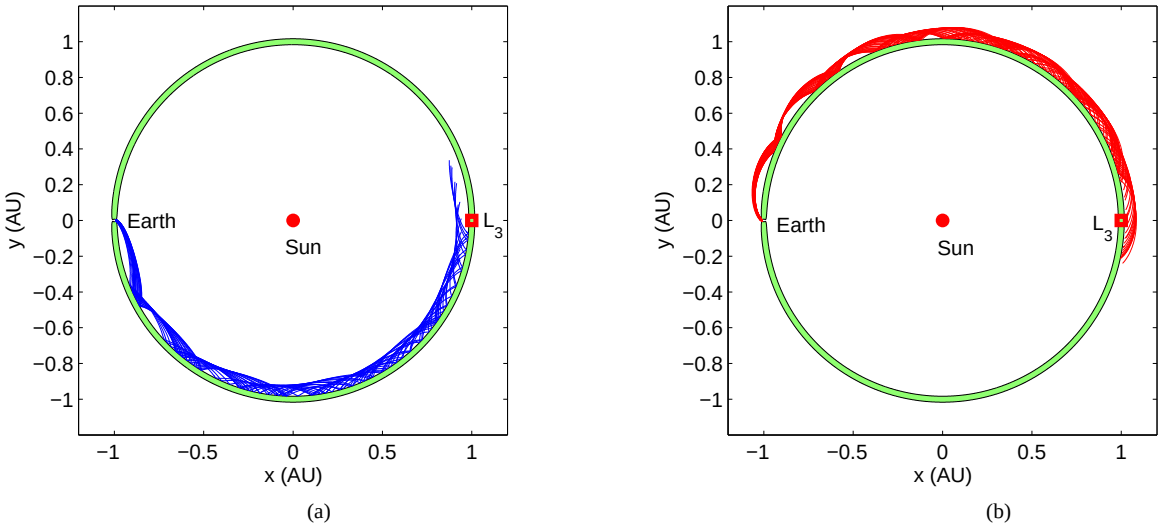

Fig. 7 A branch of the unstable manifold of one planar Lyapunov orbit around the L_1 point (a) and a branch of the unstable manifold of one planar Lyapunov around the L_2 point (b) in the Sun-Earth CR3BP.

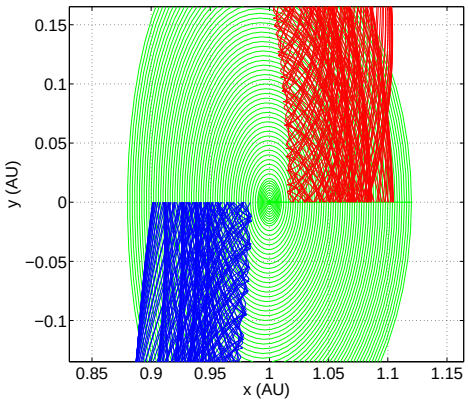

Fig. 8 Enlarged view of the area around the L_3 point of the system showing the overlap in coordinate space between an unstable invariant manifolds of L_1 (coming from below) and L_2 (coming from above) and the planar Lyapunov orbits of the L_3 family.

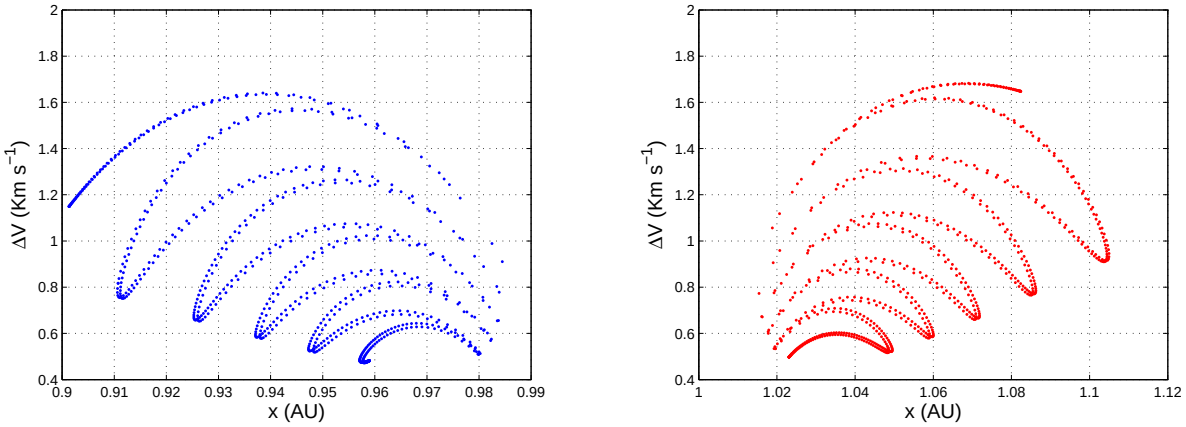

Fig. 9 Size of the insertion maneuver for a s/c traveling on the L_1 (a) and on the L_2 (b) manifold and moving onto a Lyapunov orbit of the L_3 family.

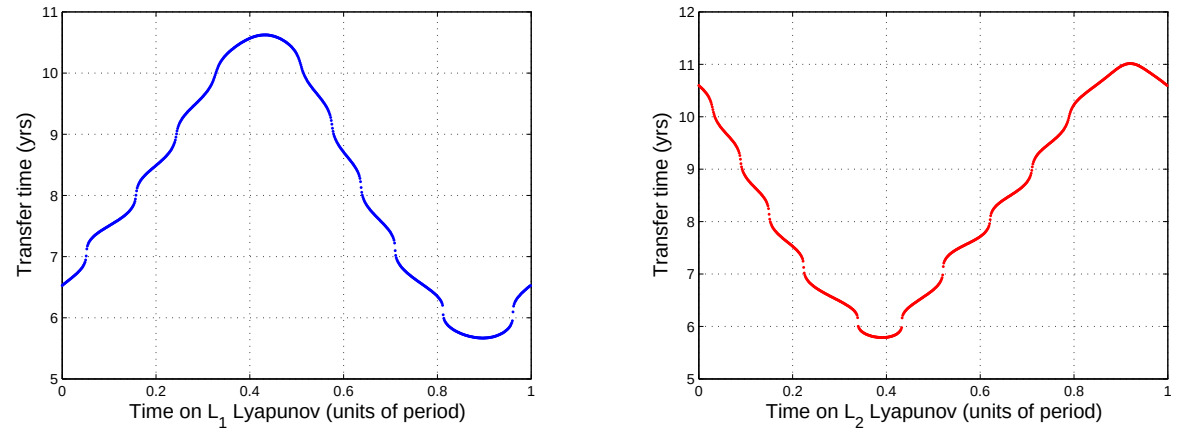

Fig. 10 Transfer times as a function of the location on the departure Lyapunov orbit (expressed in units of the period of the Lyapunov orbit) for the L_1-L_3 (a) and L_2-L_3 (b) solutions, respectively.

$$\ddot{y} = -\frac{GM_{\odot}}{r^3} y + \frac{T}{m}\alpha_y, \tag{11}$$

supplemented by the differential equation that governs the mass variation:

$$\dot{m} = -\frac{T}{g_0 I_{sp}}. \tag{12}$$

In Eqs. 10 - 12, T is the thrust provided by the engine and is the force acting on the s/c, m is the s/c mass, g_0 is the gravity acceleration at the Earth's surface, I_{sp} is the specific impulse of the engine and α_x and α_y are the x and y components of the thrust direction, i.e., the unit vector α. The trajectory is assumed to start at the surface of the Earth's sphere of influence either from L_1 or L_2 and end with the s/c at rest in L_3.

The trajectory is solved as an optimal control problem ([2,10]) consisting in finding the thrust direction α as a function of time such that the performance index is minimized. By using the Pontryagin minimum principle, the dynamical equations (Eqs. 10 - 12) are supplemented by a set of costate equations in Hamiltonian form:

$$\dot{\lambda}_{\mathbf{r}} = -\frac{\partial H}{\partial \mathbf{r}} = \left(\frac{GM_{\odot}}{r^3}\lambda_{\mathbf{v}} - \frac{3GM_{\odot}}{r^5}\lambda_{\mathbf{v}}^T\mathbf{r}\right)\mathbf{r}, \tag{13}$$

$$\dot{\lambda}_{\mathbf{v}} = -\frac{\partial H}{\partial \mathbf{v}} = -\lambda_{\mathbf{r}}, \tag{14}$$

$$\dot{\lambda}_m = -\frac{\partial H}{\partial m} = -\frac{T}{m^2} \mid\mid \lambda_{\mathbf{v}} \mid\mid, \tag{15}$$

in which $||\cdot||$ is the operator norm, and the Hamiltonian H of the system is

$$H = \lambda_{\mathbf{r}}^T \mathbf{v} + \lambda_{\mathbf{v}}^T \left(-\frac{GM_\odot}{r^3}\mathbf{r} + \frac{T}{m}\alpha \right) - \frac{T}{g_0 I_{sp}}\lambda_m, \tag{16}$$

and $\lambda_{\mathbf{r}}^T$, $\lambda_{\mathbf{v}}^T$ and λ_m are the Lagrangian multipliers (or costates) associated with position $\mathbf{r}$, velocity $\mathbf{v}$ and mass m, respectively. The optimal thrust vector α is obtained by setting $\partial H/\partial\alpha = 0$ with the normalization constraint $\alpha^T \cdot \alpha = 1$. This leads to the following expression for the optimal control $\alpha^\star$:

$$\alpha^* = -\frac{\lambda_{\mathbf{v}}}{||\,\lambda_{\mathbf{v}}\,||}, \tag{17}$$

where the minus sign follows from the Legendre-Clebsch condition (see, e.g., [2]) which guarantees that the Hamiltonian is minimized. A thrust segment is determined by Eqs. 10 to 17, given a set of initial values for states and costates. The trajectory is computed by solving the resulting nonlinear constrained optimization problem. In this study two kinds of thrust operation have been considered: one in which the thrust is assumed to be continuous throughout the transfer (optimal time, OT) and one in which a thrust-coast-thrust scheme is followed (optimal fuel, OF).

5.1 Optimal time strategy

The performance index of the parameter optimization problem is the final time $t_f(\mathbf{z})$ (to be minimized), where $\mathbf{z}$ represents the optimization parameters $\lambda_{\mathbf{r}}(0)$, $\lambda_{\mathbf{v}}(0)$ and t_f. The requirement of matching the position $\mathbf{r}(t_f)$ and the velocity $\mathbf{v}(t_f)$ of L_3 at time t_f is expressed by the constraint equalities $\mathbf{r}(t_f) - \mathbf{r}_{L_3}(t_f) = 0$ and $\mathbf{v}(t_f) - \mathbf{v}_{L_3}(t_f) = 0$, in which $\mathbf{r}(t_f)$ and $\mathbf{v}(t_f)$ are the final position and velocity of the s/c at $t = t_f$.

The transversality conditions and the final value of the Hamiltonian, which appear in the standard indirect method, are here ignored. A trial and error guess of the optimization parameters at $t = 0$ feeds the sequential quadratic programming algorithm implemented in the SNOPT ([4]) computer program. One solution of this type has been obtained by assuming a s/c with an initial mass m_0 of 500 kg, endowed with an electric engine of 3100 s specific impulse and a thrust T of 90 mN, departing from L_1. The resulting trajectory is illustrated in Fig. 11a, represented in heliocentric inertial coordinates. The refinement in the Sun-Earth CR3BP by means of the direct method provides the trajectory shown in Fig. 11b. More solutions can be obtained by continuation on the thrust, up to an upper limit for T which expresses a safety measure against collisions with the Sun. In our experiments, T has been made to vary between 20 and 100 mN. The relationship between the thrust and the TOF is shown in Fig. 12a, whereas Fig. 12b illustrates the relationship between the thrust and the percentage of mass used, separately for departures from L_1 and L_2. Finally, Fig. 13 gives the relationship between the TOF and the mass consumption. We can conclude that flying to L_3 from L_1 is cheaper and faster than from L_2. For example, a s/c with T = 90 mN reaches L_3 in 566 and 629 days, respectively from L_1 and L_2, and the mass consumption is 29% and 32% in the two cases.

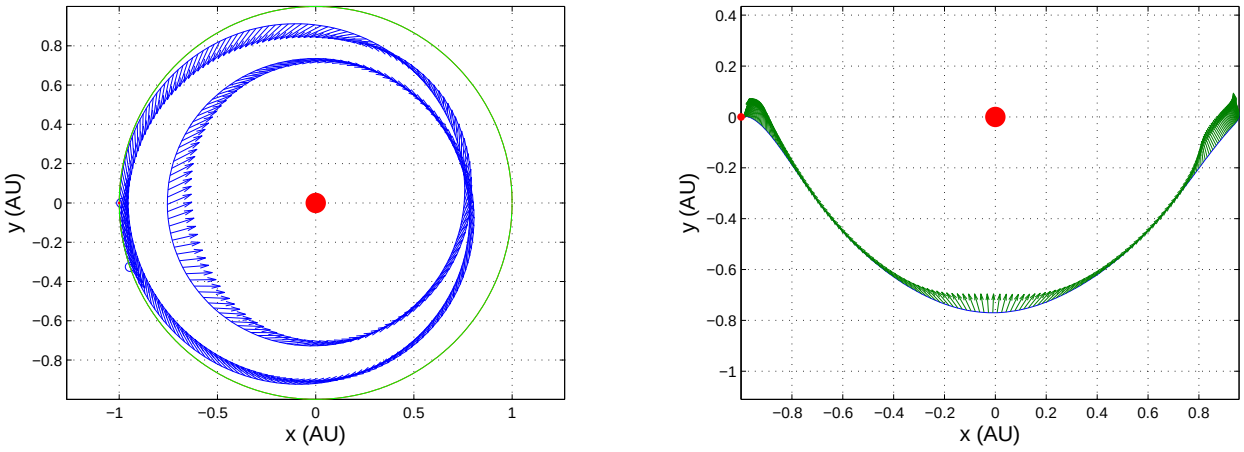

(a) (b)

Fig. 11 A trajectory to L_3 obtained by solving the time optimal control problem in the Sun-s/c two-body model with the parameters given in the text and departing from L_1 (a) and its refinement in the Sun-Earth CR3BP (b): the arrows indicate the instantaneous direction of thrust and the two empty circles show the location of the start (L_1) and end (L_3) points; the solid circles represent the Sun and the Earth.

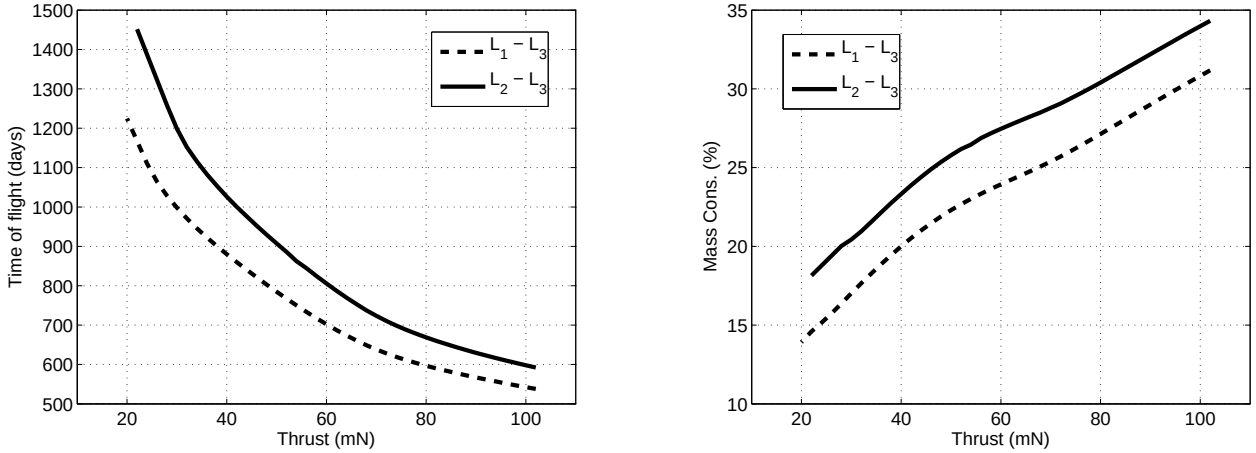

(a) (b)

Fig. 12 OT strategy: TOF (a) and mass consumption (b) as a function of thrust, separately for departures from L_1 and L_2.

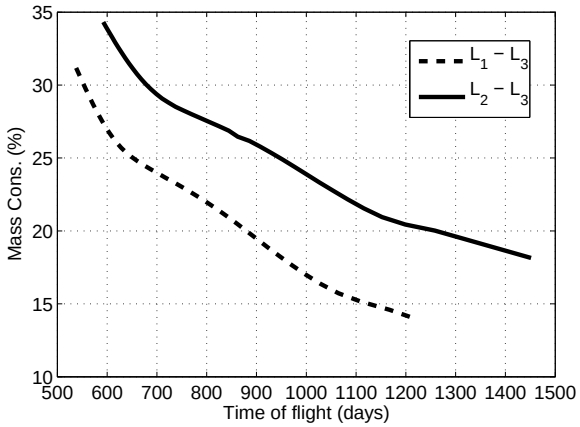

Fig. 13 OT strategy: TOF vs. mass consumption, as obtained by varying the thrust magnitude from 20 to 100 mN and considering departures from either L_1 or L_2.

5.2 Optimal fuel strategy

The performance index of the parameter optimization problem is $-m_f(\mathbf{z})$ (to be minimized), where m_f is the final fuel mass and $\mathbf{z}$ represents the optimization parameters $\lambda_{\mathbf{r}}(0)$, $\lambda_{\mathbf{v}}(0)$, $\lambda_{\mathbf{r}}[(1-p_2)t_f]$, $\lambda_{\mathbf{v}}[(1-p_2)t_f]$, p_1, p_2, and t_f: as in the previous case, t_f is the TOF, p_1 and p_2 give the duration of the first and the second thrust segments in units of the total TOF, whereas $\lambda_{\mathbf{r}}[(1-p_2)t_f]$ and $\lambda_{\mathbf{v}}[(1-p_2)t_f]$ are the initial values of the costates on the second thrust segment. The final time constraints $\mathbf{r}(t_f) - \mathbf{r}_{L_3}(t_f) = 0$ and $\mathbf{v}(t_f) - \mathbf{v}_{L_3}(t_f) = 0$ are the same as in the OT case, but now an additional requirement that the TOF is lower than a given value (of 3 years) has to be imposed in order to avoid that the solution converges to an optimal transfer orbit with two very short thrust segments and a long coast segment, in which the s/c achieves the correct phasing with respect to L_3 (and the longer the coast segment the lower the fuel consumption). With an initial mass m_0 of 500kg, a specific impulse I_{sp} of 3100s and a thrust T of 48 and 50 mN, we have computed two transfer orbits, respectively departing from L_1 and L_2: the solutions have been obtained in the Sun-s/c two-body model and then refined in the Sun-Earth CR3BP (Figs. 14 and 15).

Continuation on the thrust provides more transfer orbits. For the present case, the Sun collision avoidance places the upper limit for the thrust at 250 mN. The adopted range of variation of T is 50 to 250 mN. The relationship between thrust, TOF and mass consumption is shown in Figs. 16 and 17. Note that in this case the mass consumption is not very sensitive to thrust variations.

Finally, note that when $T = 90mN$, the OT transfer takes approximately 600 days from L_1 or L_2 with about 30% of mass consumption, whereas the OF transfer needs about 1000 days and employs 11% of the mass.

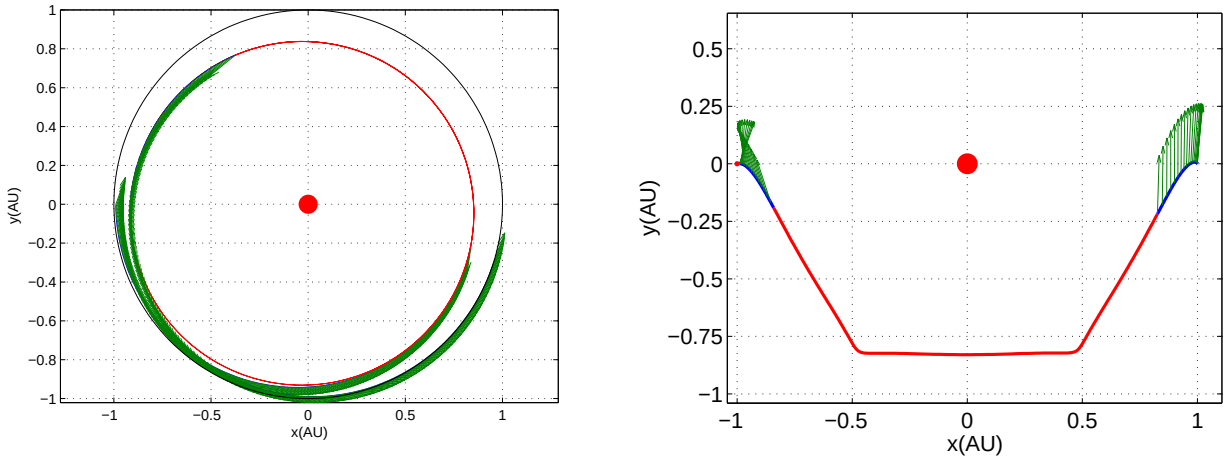

(a) (b)

Fig. 14 A thrust-coast-thrust transfer from L_1 to L_3 with T=48 mN in inertial coordinates (a) and after refinement in the Sun-Earth CR3BP (b).

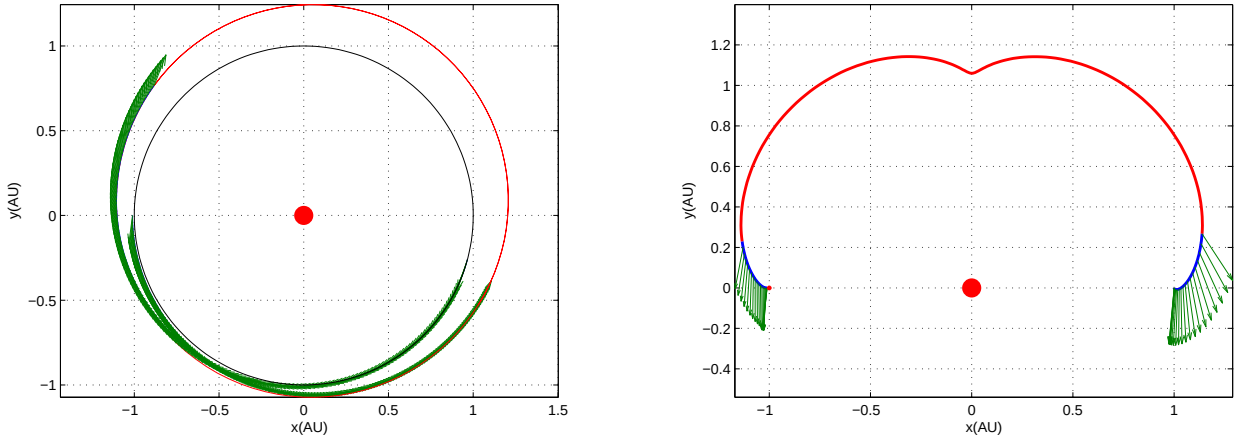

(a) (b)

Fig. 15 A thrust-coast-thrust transfer from L_2 to L_3 with T=50 mN in inertial coordinates (a) and after refinement in the Sun-Earth CR3BP (b).

6 Comparisons

In this contribution, three approaches based on the use of impulsive maneuvers have been explored to design a trajectory from the Earth's vicinity to the L_3 point of the Sun-Earth CR3BP. If a trade-off is made between ΔV budget and transfer times, the classical two-body techniques of Sect. 2 allow to reach L_3 in 2.5 years at a cost of 4.0 km s^{-1} (multi-revolution solution with $n = 2$). Trajectories assisted by planetary swingbys are generally more expensive. In particular, those based on multiple gravity assists at several different planets are not cheap enough to justify the large transfer times (e.g., $>$ 1000 days). Others, e.g., those involving one swingby at the Earth, have transfer times of only 1.5 years, but require further verification due to the low relative velocity on the incoming hyperbola. Alternative solutions based on a single Earth's swinbgy preceded and followed by a number of revolutions on appropriately tailored elliptical orbits resonant with the Earth, are characterized by ΔV budgets as low as 4.7 km s^{-1}, but have very large times of flight ($\sim$ 2300-2600 days). The third approach based on impulsive maneuvers, exploits the unstable invariant manifolds of the remaining two collinear libration points of the system (i.e., L_1 and L_2) as natural pathways to reach the area where the periodic orbits around the L_3 point reside: the TOF ranges between 5.5 and 11 years, depending on the development in space of the manifold trajectory adopted to accomplish the transfer. The cost of the insertion maneuver is between 0.5 and 1.6 km s^{-1}, but an additional budget of approximately 3 km s^{-1} should be accounted for in order to connect the invariant manifolds with the Earth through, e.g., a GTO orbit. An alternative strategy based on a different thrust concept, i.e., that provided by electrical engines, has been explored: the solution of an optimal control problem based on minimizing the TOF of a transfer in which the low-thrust propulsion is always operational (OT strategy), has provided trajectories in the

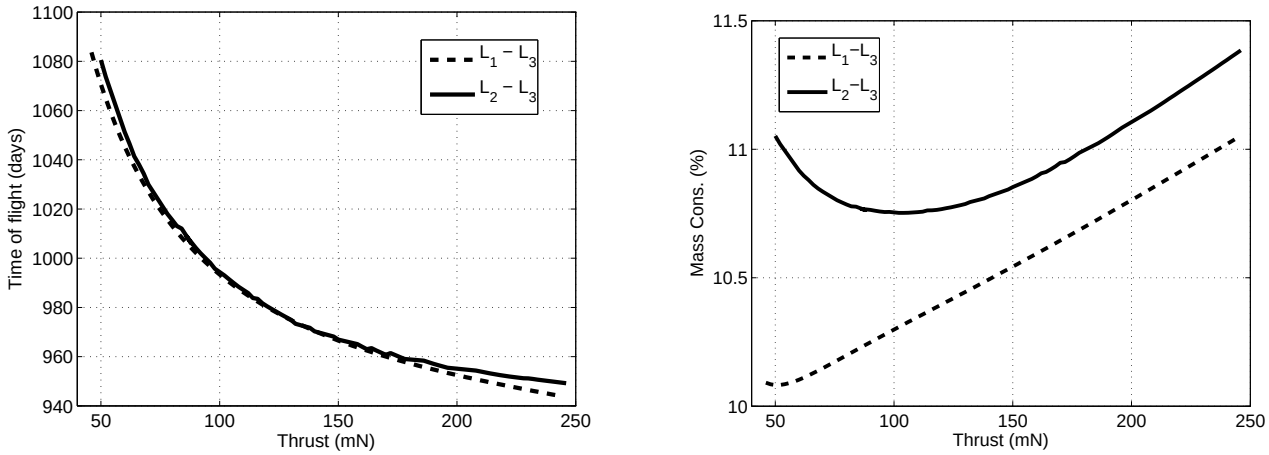

Fig. 16 OF strategy: TOF (a) and mass consumption (b) as a function of thrust, separately for departures from L_1 and L_2.

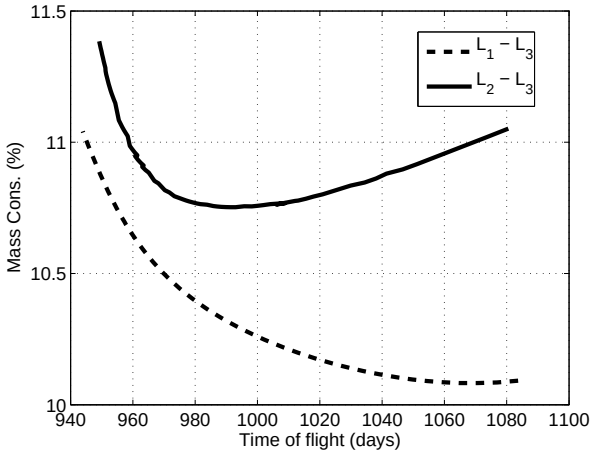

Fig. 17 OF strategy: TOF vs. mass consumption, as obtained by varying the thrust magnitude from 20 to 100 mN and considering departures from either L_1 or L_2.

Sun-s/c two-body model which reach L_3 from either L_1 or L_2 with $15 \div 30\%$ consumption of the initial mass in $550 \div 1400$ days. The solutions obtained by minimizing the fuel consumption in a thrust-coast-thrust propulsion sequence (OF strategy) are characterized by a mass consumption of $10 \div 11$ % and transfer times between 950 and 1080 days.

A global comparison among the several categories of transfers is here presented as a plot of mass consumption versus TOF (Fig. 18) for the best or the most representative solutions of each method. For the low-thrust case, the OT and OF curves correspond to departure from the more favorable location, i.e., L_1. The mass consumption of the impulsive trajectories has been obtained from the corresponding ΔV by assuming an initial s/c mass m_i of 500 kg and a specific impulse I_{sp} of 300 s and computing the ratio of final to initial mass m_f/m_i as

$$\frac{m_f}{m_i} = \exp\left(-\frac{\Delta V}{I_{sp} g_0}\right). \tag{18}$$

Fig. 18 is largely in favor of the low-thrust solutions, in either operation scheme (OT or OF) as these are characterized by much lower fuel consumption levels (10 to 30 %) than any impulsive trajectory with the same TOF (in the range, say, between 500 and 1200 days). Only the invariant manifold strategy implies similar mass budgets, but at the price of a much longer transfer duration (3800 days). Among the impulsive solutions, the single, powered gravity assist with the Earth is characterized by approximately the same TOF as the best bi-elliptic solution (which is more fuel-expensive), and is better than the multi-revolution scenario (here reported are the cases with $n = 1, 2, ..., 10$ which span a range of TOFs up to the largest transfer time of the IM solutions). However, for the feasibility of the EEL_3 trajectory, a numerical verification of the close approach phase is required, or some deep space maneuver needs to be added. This issue constitutes an interesting future development of the

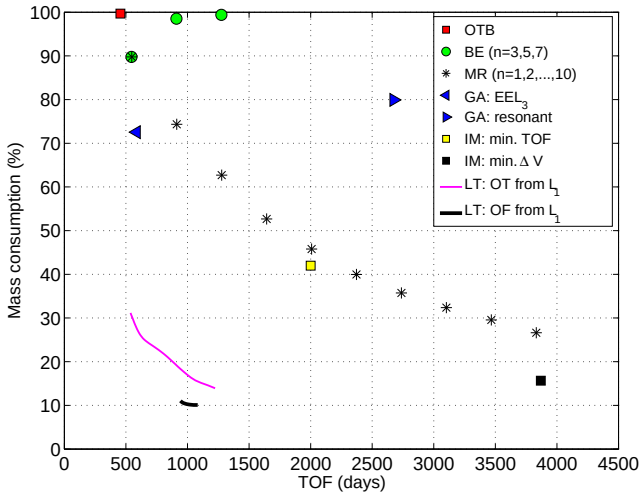

Fig. 18 Comparison among the several trajectory solutions in terms of mass consumption (% of the initial mass) and TOF (days). The mass consumption for the impulsive cases has been computed assuming a specific impulse of 300 s and an initial mass of 500 kg. The abbreviations used in the legend mean one-tangent burn (OTB), BE (bi-elliptic), MR (multi-revolution), GA (gravity assist), IM (invariant manifold), LT (low-thrust), respectively. When not explicitly specified, the values reported in the plot refer to the best case of the corresponding category.

work. The resonant orbit alternative is far too time and fuel consuming and should no longer be investigated. As for the IM solutions, two cases appear in the plot, i.e., those characterized by the smallest transfer time and the smallest maneuver size (irrespective of the departure location, i.e., L_1 and L_2), respectively: they are both characterized by lower fuel consumption than the corresponding (i.e., having the same TOF) multi-revolution trajectories (i.e., those with $n = 5$ and $n = 10$). Finally, this comparison should be considered as purely indicative and the reader should bear in mind that, for example, studying different swingby sequences or adopting different low-thrust models and parameters (i.e., specific impulse, initial mass and thrust) might lead to different trade-offs and conclusions.

7 Conclusions

The investigation here presented is a preliminary study of possible ways for a s/c to reach the L_3 point of the Sun-Earth CR3BP, based on different dynamical models (two-body problem, patched conics, three-body problem) and propulsion types (chemical, electrical): classical two-body impulsive maneuvers, optimized gravity assisted trajectories with patched conics and powered swingbys, impulsive trajectories in the Sun-Earth CR3BP exploiting invariant manifolds of libration point orbits, and different types of low-thrust transfers optimized in the two-body problem and refined in the Sun-Earth CR3BP. The comparison among the several strategies is based on a trade-off between fuel consumption and TOF and essentially favors electrical engines because these, in either operation scheme (OT or OF), are capable of taking the s/c to L_3 in the same range of times as the impulsive strategies (primarily the classical maneuvers such as bi-elliptic or multi-revolution) but with a much lower fuel expenditure (10 to 30 $\%$ vs. 70 to 99 $\%$). Only the invariant manifold strategy implies similar mass budgets, but at the price of a much longer transfer duration (3800 instead of 1000 days). This suggests that, at least under the approximations, models and parametrizations used in this study, the adoption of a low-thrust, electrical engine represents the most favorable option.

Acknowledgements M. Tantardini wishes to express his gratitude to Prof. Ron Noomen for the many helpful discussions. E. Fantino, Y. Ren and P. Pergola have been supported by the Marie Curie Actions Research Training Network AstroNet MCRTN-CT-2006-035151. This support is gratefully acknowledged. G. Gómez and J.J. Masdemont have been partially supported by the grants MTM2006-05849/Consolider, MTM2009-06973 and 2009SGR859. The authors are grateful for the valuable suggestions of the editor and two unknown reviewers. Finally, the authors acknowledge the use of EIXAM, the UPC Applied Math cluster system for research computing (see http://www.ma1.upc.edu/eixam/), and in particular Pau Roldan for providing technical support in the use of the cluster.

References

1. Barrabés, E., Ollé, M., Invariant Manifolds of L3 and horseshoe motion in the restricted three-body problem, Nonlinearity, 9, 2065-2090, 2006.
2. Brison, A.E., Ho, Y.-C., Applied optimal control, Blaisdell Publishing Company, Waltham (Massachusetts), 1969.
3. Font, J., The role of homoclinic and heteroclinic orbits in two-degrees of freedom Hamiltonian systems, Ph.D. Dissertation, Departament de Matemática. Aplicada i Analisi, Universitat de Barcelona, 1990.
4. Gill, P.E., Murray, W., Saunders, M.A., Snopt: an sqp algorithm for large-scale constrained optimization, SIAM J. Optim., 12, 979-1006, 2002.

5. Gómez, G., Koon, W.S., Lo, M.W., Marsden, J., Masdemont, J., Ross, S.D.: Connecting orbits and invariant manifolds in the spatial three-body problem, Nonlinearity, 17, 1571, 2004.
6. Hechler, M., Yanez, A., Herschel/Planck Consolidated Report on Mission Analysis FP-MA-RP-0010-TOS/GMA Issue 3.1, 2006.
7. Hou, X., Tang, J., Liu, L.: Transfer to the collinear libration point L_3 in the Sun-Earth+Moon system, Nasa Technical Report 20080012700, 2007.
8. Lo, M.W., Williams, B.G., Bollman, W.E., Han, D., Hahn, Y., et al.: Genesis Mission Design, AIAA Space Flight Mechanics, Paper No. AIAA 98-4468, 1998.
9. Koon,W.S., Lo, M.W., Marsden, J.E., Ross, S.D.: Heteroclinic connections between periodic orbits and resonance transitions in celestial mechanics, Chaos 10 (2), 427-469, 2000.
10. Senent, J., Ocampo, C., Capella, A., Low-thrust variable-specific-impulse transfers and guidance to unstable periodic orbits, J. Guid. Contr. Dyn. 28, 280-290, 2005.
11. Szebehely, V., Theory of orbits, Academic Press, New York (Massachusetts), 1967.
12. Tantardini, M.: Transfer strategies to the L_3 libration point of the Sun-Earth system, MS Thesis, Aerospace Engineering, Delft University of Technology, Delft, The Netherlands, 2009.
13. Vallado, D.A., Fundamentals of astrodynamics and applications, Microcosm Press, Hawthorne (California), 2007.